Penerbit Akademia Baru

Journal of Advanced Research Design

Journal homepage:
https://akademiabaru.com/submit/index.php/ard
ISSN: 2289-7984

Synergistic Integration of Modular Four-Channel 50 kW WPT System: Enhancing Fast EV Charging and PMSM Drive Integration

Kambampati Lakshmi[1,2], T. Vijay Muni[1], A.S. Veerendra[3,4,*], D. Ravi Kishore[5], Norazlianie Sazali[6,7], Kumaran Kadirgama[7,8,9]

[1] Department of Electrical and Electronics Engineering, Koneru Lakshmaiah Education Foundation, Vaddeswaram, Andhra Pradesh 522302, India
[2] Department of Electrical and Electronics Engineering, Aditya University, Surampalem, Andhra Pradesh 533437, India
[3] Department of Electrical and Electronics Engineering, Manipal Institute of Technology, Manipal Academy of Higher Education, Manipal, Karnataka 576104, India
[4] Research fellow, Department of Electrical and Electronics Engineering, INTI International University, Putra Nilai,71800 Nilai, Negeri Sembilan, Malaysia
[5] Department of Electrical and Electronics Engineering, Godavari Global University, Rajamahendravaram, Andhra Pradesh 533296, India
[6] Faculty of Mechanical and Manufacturing Engineering, Universiti Tun Hussein Onn Malaysia, Parit Raja, 86400 Batu Pahat, Johor, Malaysia
[7] Centre of Excellence for Advanced Research in Fluid Flow (CARIFF), Universiti Malaysia Pahang Al-Sultan Abdullah, 26600 Pekan, Pahang, Malaysia
[8] Faculty of Mechanical & Automotive Engineering Technology, Universiti Malaysia Pahang Al-Sultan Abdullah, 26600 Pekan, Pahang, Malaysia
[9] College of Engineering, Almaaqal University, Basra 61003, Iraq

ARTICLE INFO

Article history:
Received 28 February 2025
Received in revised form 17 March 2025
Accepted 14 July 2025
Available online 25 July 2025

Keywords:
Wireless EV charging; high-power; modular; decoupled coil design; misalignment tolerance; PMSM drive

ABSTRACT

This paper presents an innovative approach to electric vehicle (EV) charging and propulsion system integration through the development of a Modular Four-Channel 50 kW Wireless Power Transfer (WPT) System with Decoupled Coil Design. The system architecture is designed to facilitate rapid charging of EV batteries while also enabling a seamless transition to a Permanent Magnet Synchronous Motor (PMSM) drive application post-charging. The decoupled coil design ensures efficient power transfer while minimizing electromagnetic interference. Leveraging this integrated solution, the charging process is optimized for speed and reliability, enhancing the EV user experience. Furthermore, the seamless transition to the PMSM drive application allows for immediate utilization of the charged EV battery for propulsion, ensuring maximum efficiency and functionality. The system delivers 50 kW power with 97% DC-to-DC efficiency over a 200 mm airgap and demonstrates balanced tolerance to misalignment. MATLAB/simulation validation demonstrates the effectiveness of the proposed system in achieving fast EV charging and smooth integration with the PMSM drive application, thereby offering a promising solution for future electric vehicle technology advancement.

1. Introduction

EV production has expanded internationally in recent years, driven by concerns about energy scarcity and pollution. It takes a long time to charge an electric vehicle's battery compared to filling

* *Corresponding author*
E-mail address: veerendra.babu@manipal.edu

https://doi.org/10.37934/ard.139.1.119

up a gasoline-powered vehicle [1] and conventional conductive charging methods for EVs use thick gauge wires that are both hazardous and difficult to manage. The aesthetic, safety, convenience and completely automated charging process benefits of (WPT), which primarily refers to inductive power transfer (IPT), have put it in the spotlight as a viable alternative to conductive charging in recent years [2]. While WPT has many potential uses, one major drawback is the lengthy time it takes to charge some types of electric vehicles and buses (e.g., public transportation) [3]. The only way to shorten charging durations is to use high-power input [4]. Thus, there has been an uptick in the need for high-power WPT technology [3,5,6].

Raising the power capacity of WPT systems is quite difficult because of the voltage and current constraints of power electronic components. In order to avoid employing wide-bandgap devices like Silicon-Carbide (SiC), some academic and commercial organizations have suggested 50 kW or more WPT systems [7-9]. However, gadgets will continue to inhibit the advancement of system power capabilities. Also, the insulation of resonant parts and voltage stress are the obstacles to high-power wireless charging in the real world of electric vehicles with limited interior space. Many other ways to get beyond the restrictions of the device and the resonant element have been suggested as solutions to the aforementioned difficulty, with the goal of increasing the power capacity of the WPT system.

A cascaded multilevel inverter has been suggested as a means to enhance the power level in the WPT system [10-13]. Due to the inverters' series connection, however, the cascaded structure of the multilayer converter has poor dependability. To boost the transmitter current and enhance the WPT system's dependability, it is suggested to use several inverters that are linked in parallel using low-current semiconductor devices [14]. Insulation design is made more challenging by the high voltage stress on the resonant parts caused by the high transmitter current. Due to the fact that both the cascade and parallel connection techniques only use a single transmitting coil, the system only has one outlet for power transmission. Because of their shared issue with unreliability and malfunction, they are all vulnerable to failure. Ahn *et al.,* [15] and Liu *et al.,* [19], the authors suggest WPT systems that use several transmitters and receivers to send and receive power. A decrease in voltage stress on resonant parts and an improvement in the system's power capabilities make this possible. However, there's not insignificant cross-coupling between different power transfer channels, which leads to uneven power distribution and circulation across channels and drastically reduces the efficiency and capacity of power transfer [15]. Coupling two magnetic couplers is achieved [16,17] by combining polarized and non-polarized coils. Still, the two-channel system can only broadcast 4.73 kW and because the technology isn't expandable, there's no way to increase the transmission power capabilities via modularization. To solve the problem of magnetic coupling between couplers, the authors of Shijo *et al.,* [18] and Liu *et al.,* [19] use a technique that involves moving the polarized coils of the two couplers apart. The transmitting power of the two channel systems is 44 kW and 7 kW, respectively. This approach can be scaled up or down, but there will be a limit to how much space each module can take up. On top of that, electric vehicle parking becomes more complicated in real-world scenarios because of the polarised coils' properties, which cause the multi-channel systems discussed before to have an uneven system misalignment tolerance in the horizontal and vertical directions. To facilitate rapid electric vehicle charging, this study proposes a modular four-channel WPT system using a decoupled coil architecture.

The modular four-channel 50 kW WPT system addresses voltage stress, misalignment tolerance, efficiency and scalability to improve high-power wireless power transfer (WPT) systems. Real-world EV charging is less efficient with single-channel WPT systems due to high voltage stress, power scalability and misalignment. The suggested system's decoupled coil design and modular architecture minimize voltage stress, increase power transfer efficiency and improve misalignment tolerance. The

suggested system decouples channels, assuring independent channel operation and uniform power distribution, unlike multi-channel WPT systems, which have cross-coupling and power imbalances. Although many high-power WPT systems use expensive Silicon Carbide (SiC) devices, the suggested system uses low-power silicon-based devices to provide 50.8 kW and 97% DC-to-DC efficiency. EV parking and charging are also complicated by standard multi-channel WPT systems' unequal misalignment tolerance. The suggested system balances lateral and vertical misalignment tolerance using a rotationally symmetric four-channel magnetic coupler. Another benefit is its smooth connection with a Permanent Magnet Synchronous Motor (PMSM) drive, which regenerates energy while braking to increase EV range and sustainability. This WPT system optimises charging and propulsion, making it a more practical and future-ready EV alternative than others. The study's contribution to wireless EV charging will be strengthened by including these comparative benefits in the literature evaluation.

The four WPT modules that make up the modular system's four parallel power transfer channels are similar in every respect. Each module has a main power factor correction (PFC) rectifier, an inverter, a set of coils for the transmitter and receiver and a secondary rectifier. Because all four modules have the same power capacity, the total transmitted power is equal to four times that amount. The primary challenge is the short range of electric vehicles caused by the finite power of batteries. Driving range is directly proportional to battery size and capacity; increasing the battery rating is one apparent way to accomplish this, but doing so would raise the vehicle's weight and the expense of electric vehicles in general [20].

The whole driving cycle, including acceleration, coasting and de-acceleration, puts an electric motor used in a vehicle under varied dynamics. The motor is turned on with a positive peak torque while the driving cycle is in acceleration mode and a negative peak torque when the cycle is in de-acceleration [21]. When in acceleration mode, power is drawn out of the power supply. When the car is in de-acceleration mode, the energy comes from the battery. To slow down, the brakes are applied, which is represented by the negative torque. In this case, the vehicle's kinetic energy is redirected to the battery, causing the battery's state of charge to escalate. This energy regeneration is a great way to increase the electric vehicle's range [22,23]. As the motor decelerates, its stored kinetic energy is directed by the current-controlled VSI, which in turn powers the permanent-magnet synchronous motor [24]. Our primary goal in this project is to design a system for LEVs that use batteries to power the engine. Permanent magnet synchronous motors are highly regarded for their many advantageous features, including their simple and sturdy design, lack of a permanent magnet rotor, lossless rotor, almost nil cogging torque, affordable price and dependable operation [25,26]. Thus, it offers great promise as an alternative to induction motors (IMs) in EVs and other vehicles with variable speed control drives. Compared to IM and PMSM, the energy conversion efficiency of permanent magnet synchronous motors is greater [27,28].

There are a few drawbacks to consider, such as a poor power factor, significant core loss and strong torque ripple. An EV is one of the major uses of a permanent magnet synchronous motor gaining prominence. A permanent magnet synchronous motor is indicated for use in a propulsion system [29]. This paper proposes the design the concept of electric vehicle system modelling and study of a PMSM machine, which encompasses modelling the vehicle's acceleration, range and analysis of various driving cycles, is carried out. Besides, the study introduces a novel approach to address the challenges of high-power wireless charging in electric vehicles by proposing a modular four-channel WPT system with a decoupled coil design. This system comprises four parallel power transfer channels, each consisting of a complete WPT module. By leveraging this modular architecture, the system achieves faster charging while mitigating issues related to power transfer imbalance and coil misalignment tolerance. The research emphasizes the importance of extending

the operating range of electric vehicles without significantly increasing battery size and weight. It discusses how energy regeneration during deceleration, controlled by a current-controlled Voltage Source Inverter (VSI) powering a PMSM, can augment the driving range of EVs. This focus on enhancing EV driving range contributes to the overall sustainability and practicality of electric transportation.

Furthermore, the study highlights the significance of PMSMs in electric vehicle propulsion systems, noting their advantages such as simplicity, efficiency and reliability. It discusses the use of bi-directional buck-boost converters to enhance the performance of battery-powered PMSMs during regenerative braking. Additionally, it underscores the ongoing research and development efforts aimed at optimizing PMSM design and control strategies for EV applications.

2. Methodology

2.1 System Configuration

The proposed synergistic integration comprises a modular four-channel 50 kW WPT system for fast EV charging and PMSM drive integration. The WPT system features four parallel power transfer channels, each capable of delivering 50 kW of power. Each channel consists of a Primary PFC rectifier, an inverter, transmitter and receiver coils and a secondary rectifier, facilitating efficient wireless power transmission. The modularity of the system ensures scalability and ease of maintenance. Concurrently, the PMSM drive system, seamlessly integrated into the EV's propulsion system, includes the PMSM itself, providing high-efficiency propulsion power with superior torque density. This integration streamlines EV operation while maximizing energy efficiency and facilitating rapid charging, enhancing the overall performance and sustainability of electric vehicles.

2.2 Modular Circuit Design

The four-channel WPT system that is being suggested uses identical circuit modules for each channel, as can be seen in Figure 1. This diagram presents the overall system architecture, showing four parallel power transfer channels that ensure scalable and high-power wireless charging. Each channel consists of a primary PFC rectifier, an inverter, transmitter and receiver coils and a secondary rectifier, which work together to facilitate efficient wireless energy transfer. Equipped with compensation networks, a main side high-frequency inverter, a grid-side PFC rectifier and a secondary side high-frequency rectifier make up the circuit module. Figure 10 shows the schematic design of the circuit module, using Channel 1 as an example. The proposed four-channel magnetic coupler's inter-channel decoupling is tested by simulations utilising the 3-D Finite Element Method (FEM). There are a total of 28 coupling coefficients in the coupler, which is caused by the 8 inductive coils (Lp1~ Lp4 and Ls1 Ls4). Out of these, four are for power transmission (kp1_s1, kp2_s2, kp3_s3 and kp4_s4) and there are 24 for interference (kpi_sj, kpi_pj and ksi_sj, where i j). In a simulated setup with a 200 mm air gap between the main and secondary sides, the coupling coefficient kp1_s1 for power transmission is 0.261 and the interference coefficients across channels are close to zero, according to the data. Under aligned circumstances, inter-channel decoupling is therefore accomplished. Analysing the misalignment performance further, we find that the suggested four-channel magnetic coupler outperforms conventional single-channel systems in terms of balanced lateral (X-axis) and vertical (Y-axis) misalignment tolerance.

The modular four-channel 50 kW WPT system and the PMSM drive are a revolutionary approach to EV charging and propulsion systems. The WPT system ensures precise positioning for optimal power transfer efficiency, while the PMSM drive provides optimal propulsion performance during

subsequent journeys. The main PFC rectifiers in the WPT system change the AC power that comes in from the grid into high-quality DC power. Inverters then efficiently change the DC power into high-frequency AC signals that can be sent wirelessly. The transmitter coils embedded within the charging pad emit these AC signals, generating a magnetic field that induces a voltage in the receiver coils mounted on the underside of the EV. The secondary rectifiers in the EV's charging system convert the received AC signals back into DC power, directed to the vehicle's onboard battery pack. The modular design of the WPT system enhances reliability and fault tolerance, as it can dynamically adapt to changes in environmental conditions or charging requirements. During acceleration, the PMSM delivers precise torque output, providing a dynamic driving experience that rivals conventional internal combustion engine vehicles. The sophisticated control algorithms optimize energy consumption and driving dynamics, maximizing both range and performance. Crucially, the PMSM drive system transitions into regenerative braking mode during deceleration or braking manoeuvres, harnessing kinetic energy from the vehicle's motion and converting it back into electrical power. This process extends the EV's driving range, improves overall energy efficiency, reduces brake wear and enhances environmental sustainability and operational cost-effectiveness. Through the synergistic integration of the modular WPT system and the PMSM drive, this integrated solution offers numerous benefits to EV owners, operators and society as a whole. These benefits include:

i. The WPT system eliminates the need for physical cables and connectors, simplifying the charging process. The modular design allows for flexible deployment in various locations, including residential garages, public parking lots and commercial charging stations. The high efficiency of both the WPT system and the PMSM drive minimizes energy losses during charging and propulsion, reducing overall electricity consumption and carbon emissions. The regenerative braking capability further enhances energy efficiency by recapturing kinetic energy that would otherwise be lost as heat. The robust design and fault-tolerant operation of the integrated system ensures reliable performance under diverse operating conditions, including extreme temperatures, weather conditions and terrain. The modular architecture allows for easy maintenance and scalability, minimizing downtime and optimizing system longevity.
ii. Performance: The seamless integration of the PMSM drive system delivers responsive and exhilarating driving dynamics, with instant torque delivery and smooth acceleration. The regenerative braking system enhances vehicle control and stability while maximizing driving range, resulting in an engaging and enjoyable driving experience for EV enthusiasts.

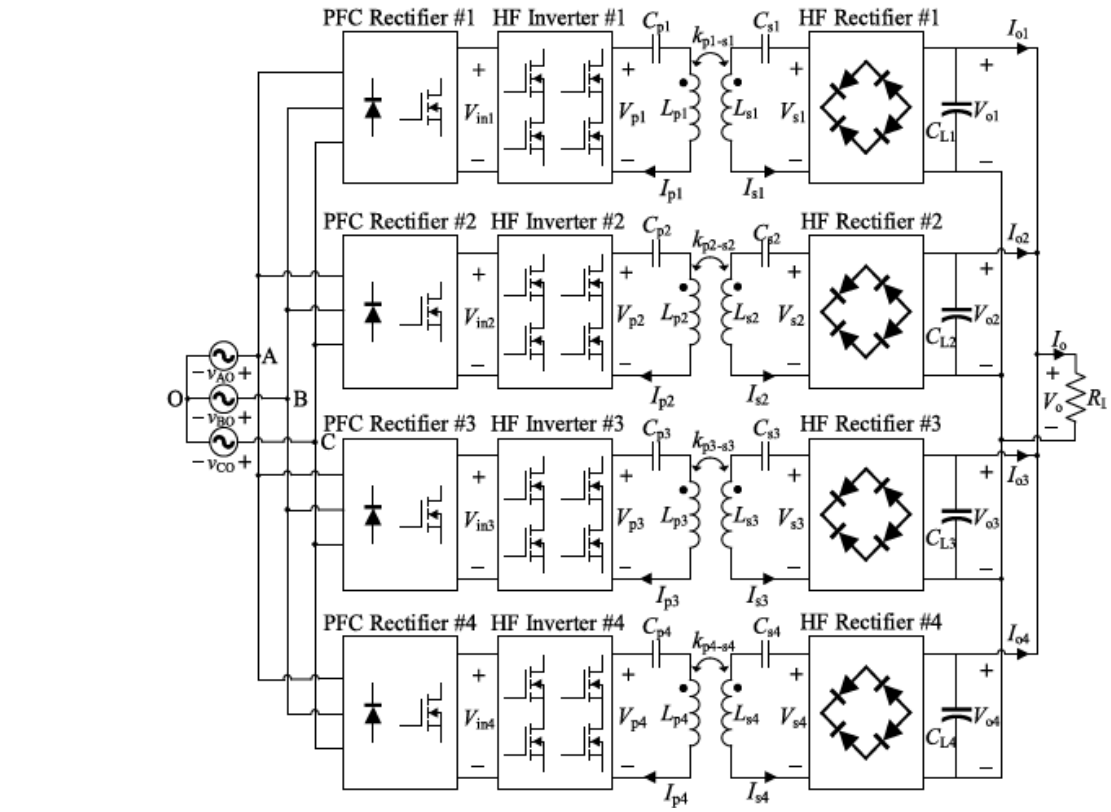

(a)

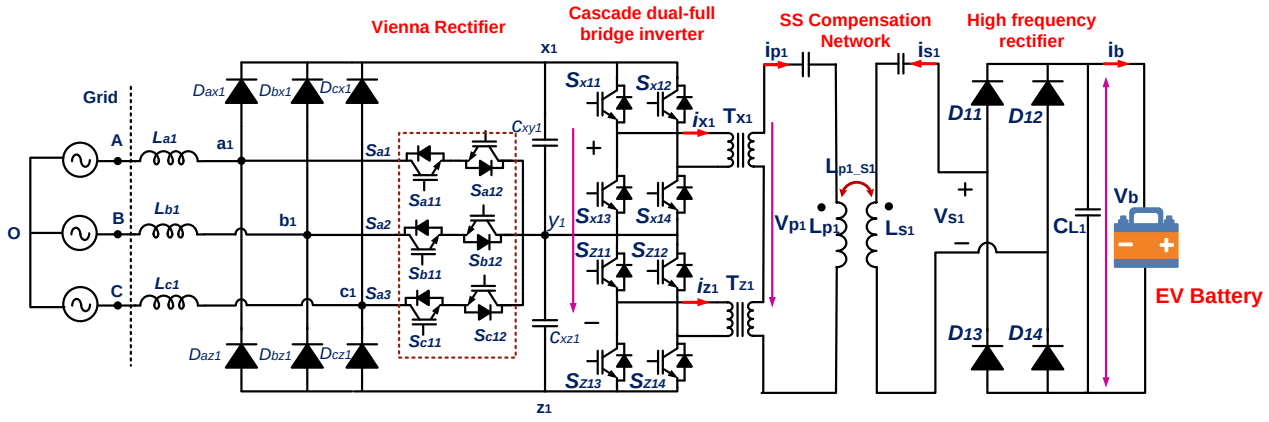

(b)

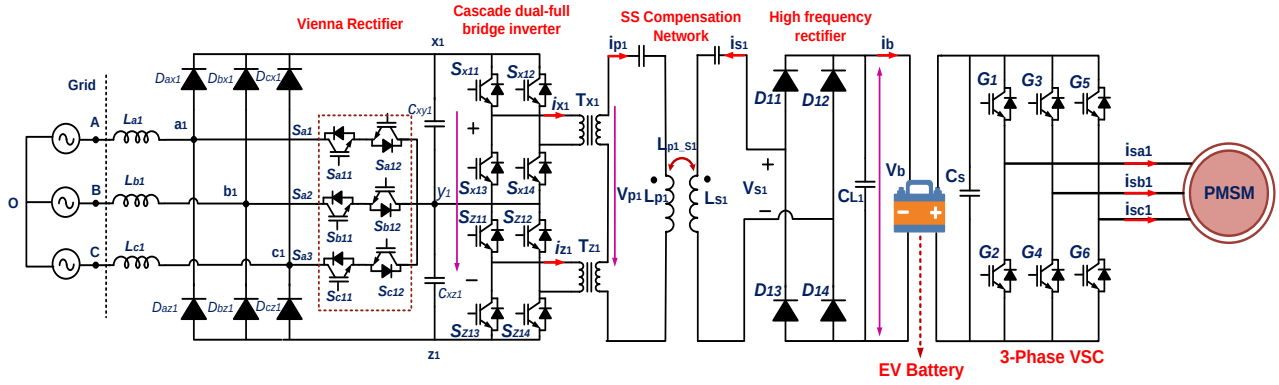

(c)

Fig. 1. (a) Block diagram of modular four-channel WPT system (b) Schematic diagram of the circuit module for EV battery charging (c) Schematic diagram of the circuit module for PMSM drive from EV battery

2.3 Gird-Side PFC Rectifier

A three-phase power factor enhancement is provided by the Vienna rectifier, which also offers several other benefits, such as sinusoidal input current, a power factor that is almost one and minimal harmonic distortion [30,31]. A number of benefits are also associated with it, including a high efficiency rate, low voltage stress and a low power loss rate [30]. Customers' electricity bills and air pollution are both helped by the Vienna rectifier. Very high switching frequencies (around 100 kHz) are used in Vienna rectifiers [32]. When the switching frequency is high, switching losses are significant and the sustainability of the switches is poor. While the Vienna rectifier makes use of two output capacitors, our suggested architecture makes use of a single one [30,32]. The Vienna control architecture is intricate and there are severe limitations on reactive power production. For reaching the unity power factor, it is very appealing. Due to its reduced number of diodes and ease of implementation, our suggested modified Vienna rectifier is ideal. To contrast with the Vienna rectifier, we used a switching frequency of 21 kHz here, which is quite low. Since the switching losses are reduced at this lower switching frequency, the efficiency is increased. Included in our straightforward and dependable controller design are a handful of logic gates, linear components and a proportional integral (PI) controller. The power factor and output DC voltage may be adjusted. The rectifier placed on the grid side is a Vienna rectifier. The rectification efficiency, power density and size of the passive components are all quite modest in a Vienna rectifier [33]. Since the rectifier's voltage stress is only half of its DC output voltage (Vin1 in Figure 4), it is able to produce a greater DC voltage. Using a high-voltage DC bus to reduce power coil current is helpful for the circuit's later stages. Lower power coil loss and more efficient energy transfer are the results of setting the power coil's quality factor. Discussion of the Vienna rectifier's operating principle and control approach is beyond the scope of this publication. The voltage relationship is shown in Figure 2 and it may be used to explain the post-stage circuit. Essentially, the output of the Vienna rectifier is the same as two equal-amplitude series DC voltage sources as in Eq. (1):

$$V_{xy1} = V_{yz1} = \frac{1}{2} V_{in1} \tag{1}$$

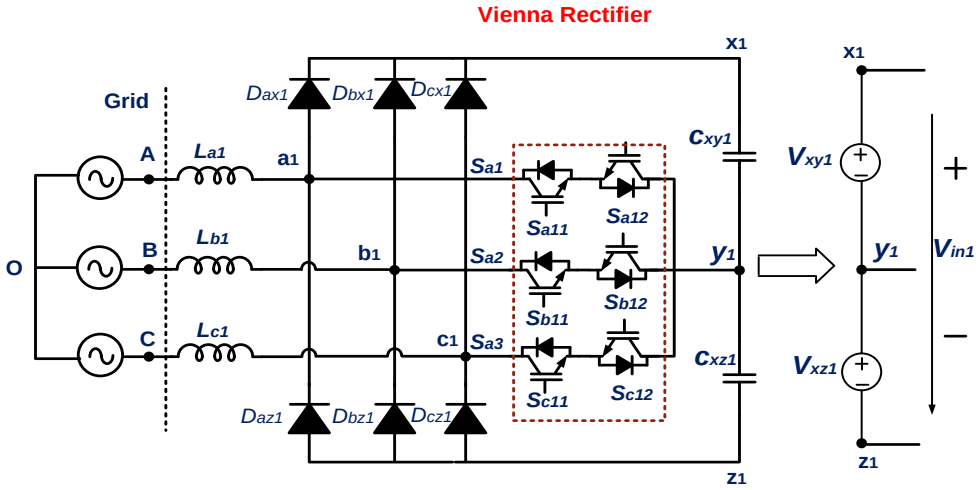

Fig. 4. Output equivalent model of Vienna rectifier

The Vienna rectifier is a three-phase AC-to-DC power conversion topology that is widely used for its high PFC and low harmonic distortion characteristics. The operation of the Vienna rectifier involves several important formulas related to its performance and control.

2.3.1 Increased surface area

For a balanced three-phase system, the phase voltages can be represented as in Eqs. (2) to (4):

$$V_{an}(t) = V_m \sin(\omega t) \quad (2)$$

$$V_{bn}(t) = V_m \sin\left(\omega t - \frac{2\pi}{3}\right) \quad (3)$$

$$V_{cn}(t) = V_m \sin\left(\omega t - \frac{2\pi}{3}\right) \quad (4)$$

Where, V_m is the peak phase voltage, ω is the angular frequency and t is time. The corresponding line currents (assuming unity power factor) can be represented as in Eqs. (5) to (7):

$$I_a(t) = I_m \sin(\omega t) \quad (5)$$

$$I_b(t) = I_m \sin\left(\omega t - \frac{2\pi}{3}\right) \quad (6)$$

$$I_c(t) = I_m \sin\left(\omega t - \frac{2\pi}{3}\right) \quad (7)$$

where I_m is the peak phase current.

2.3.2 DC output voltage

The average DC output voltage Vdc of the Vienna rectifier can be approximated by Eq. (8):

$$V_{dC} = \frac{3\sqrt{3}}{\pi} V_{LL} \cos(\phi) \quad (8)$$

Where, V_{LL} is the RMS line-to-line input voltage and ϕ is the phase angle between the input voltage and current (ideally zero for unity power factor).

2.3.3 Power factor correction

The power factor PFPF is given by the ratio of real power P to apparent power S as in Eq. (9):

$$PF = \frac{P}{s} = cos(\phi) \quad (9)$$

For a unity power factor, ϕ=0 and PF=1.

2.3.4 Input current harmonic distortion

Total harmonic distortion (THD) of the input current is a measure of the harmonic content and is given in Eq. (10):

$$THD = \sqrt{\Sigma_{n=2}^{\infty} \left(\frac{I_n}{I_1}\right)^2} \quad (10)$$

Where, In is the RMS value of the nth harmonic component of the input current and $I1$ is the RMS value of the fundamental component of the input current.

2.3.5 Inductor design

The inductance L required for the boost inductor in each phase can be estimated based on the desired ripple current ΔIL and switching frequency and is shown in Eq. (11):

$$L = \frac{V_{dC} \cdot D \cdot (1-D)}{f_s \cdot \Delta I_L} \quad (11)$$

Where, D is the duty cycle of the PWM signal.

2.3.6 Capacitor design

The DC bus capacitor C is designed to smooth the output voltage and can be estimated by Eq. (12):

$$C = \frac{I_{dC}}{2 \cdot f_{ripple} \cdot \Delta V_{dc}} \quad (12)$$

Where, I_{dC} is the DC output current, f_{ripple} is the ripple frequency (typically twice the line frequency for a three-phase rectifier) and ΔV_{dc} is the allowable voltage ripple on the DC bus.

2.3.7 RMS current in components

The RMS current through the diodes and switches can be estimated as follows in Eq. (13) and (14), respectively:

i. For diodes in each phase leg:

$$I_{DRMS} = \sqrt{\frac{1}{T}\int_0^T i_D^2(t)\,\mathrm{d}t} \quad (13)$$

ii. For switches in each phase leg:

$$Is_{RMS} = \sqrt{\frac{1}{T}\int_0^T i_S^2(t)\,\mathrm{d}t} \quad (14)$$

Where, (t) and $i_S^2(t)$ are the instantaneous currents through the diodes and switches, respectively and T is the period of the switching cycle.

2.4 Primary Side High-Frequency Inverter

The inverter's current capacity is 25% of the single-channel systems at the same power level in the proposed modular four-channel system. A cascaded dual-full bridge inverter is used to simultaneously lower the devices' voltage stress (Figure 10). The two full-bridge inverters in Figure 2 take half of the DC bus voltage Vin1 from the DC sources Vxy1 and Vyz1. The voltage stress on power components is reduced by half compared to a conventional full-bridge inverter by virtue of the cascaded architecture. A silicon-based MOSFET with a 650 V withstand voltage is a cost-effective choice for the 800 V DC bus voltage and may be used in both the Vienna rectifier and the inverter. A single inverter typically needs SiC devices to reach an 800 V input and output voltage level. This research demonstrates that by combining a Vienna rectifier with a cascaded inverter, Si devices may attain the same voltage level. Furthermore, by combining the Vienna PFC rectifier with cascaded dual full-bridge inverters, we can achieve balanced input voltages for each inverter. This is because the Vienna rectifier has a natural midpoint for its output and unlike previous approaches that relied on cascade inverters to generate high power, our method eliminates the issue of device damage caused by inconsistent voltage stress on the inverter's switching devices. The cascaded dual-full bridge inverter uses high-frequency transformers Tx1 and Tz1 (turn ratio 1:1) to cascade the output of the upper and lower inverters instead of two separate sources of input voltage Vxy1 and Vyz1, which share a common point y1. Otherwise, Vxy1 and Vyz1, which are DC voltage sources, might be short-circuited in certain switching states. The inverter and post-stage circuit are electrically isolated, which is another advantage of using high-frequency transformers. Both full-bridge inverters have their switch driving signals configured to be identical. As a result, the cascaded dual-full bridge inverter's output voltage vp1 is double that of a single full-bridge inverter's output voltage vx1 or vz1 in Eqs. (15) and (16):

$$v_{P1} = 2v_{x1} = 2v_{z1} \tag{15}$$

$$i_{P1} = i_{x1}=i_{Z1} \tag{16}$$

Both the Vienna rectifier and the cascaded dual-full bridge inverter use Infineon silicon-based MOSFETs. The 650 V rating of the device is more than enough for half of the 400 V maximum DC bus voltages. For each switch of the dual-full bridge inverter, two devices with an ON-state resistance of 80 mΩ in TO-247 housings are used in parallel to attain reduced conduction losses.

2.5 Working Operation PMSM Drive System

The integration of a PMSM drive with an EV battery involves a seamless combination of several key components to achieve efficient propulsion. The EV battery pack, typically composed of lithium-ion cells, serves as the primary energy source, providing DC power to the system as shown in Figure 5. This DC power is converted into three-phase AC power by an inverter, which is a crucial component in the drive train. The inverter uses pulse-width modulation (PWM) to precisely control the frequency and amplitude of the AC power supplied to the PMSM, enabling accurate control of the motor's speed and torque. The PMSM itself is known for its high efficiency, high power density and excellent torque characteristics, making it ideal for EV applications. During vehicle operation, the PMSM converts the electrical energy from the inverter into mechanical energy, propelling the vehicle. The motor's rotor, embedded with permanent magnets, interacts with the rotating magnetic field produced by the stator windings, generating torque. The motor's performance is continuously monitored and

adjusted by the vehicle's control system to optimize efficiency and response to driving conditions. Additionally, the system incorporates regenerative braking, where the PMSM acts as a generator during deceleration, converting kinetic energy back into electrical energy, which is then fed back to recharge the EV battery. This process not only enhances the vehicle's range but also improves overall energy efficiency. The combined operation of the EV battery, inverter and PMSM provides a robust and efficient drive train solution, ensuring smooth, responsive and energy-efficient propulsion for electric vehicles.

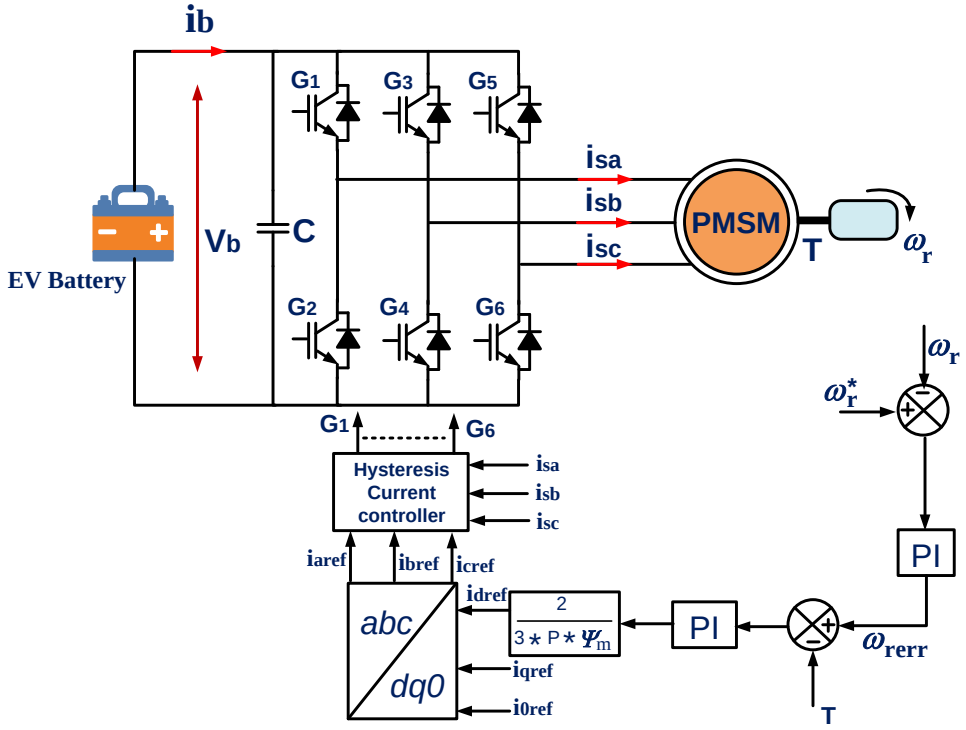

Fig. 5. Layout of battery fed for PMSM drive system

2.5.1 DC-DC converter efficiency (η_{DC-DC}) (Eq. 17):

$$\eta_{DC-DC} = \frac{P_{out,DC}}{P_{in,DC}} \times 100\% \tag{17}$$

Where, $P_{out,AC}$ is the output power of the DC-DC converter. $P_{in,DC}$ is the input power to the DC-DC converter.

2.5.2 Inverter efficiency (Eq. 18):

$$(\eta_{inverter}): \eta_{inverter} = \frac{P_{out,AC}}{P_{in,DC}} \times 100\% \tag{18}$$

Where, $P_{out,AC}$ is the output power of the inverter. $P_{in,DC}$ is the input power to the inverter.

2.5.3 Motor efficiency (η_{Motor}) (Eq. 19):

$$\eta_{Motor} = \frac{P_{out,Mechanical}}{P_{in,Electrical}} \times 100\% \tag{19}$$

Where, $P_{out,Mechanical}$ is the mechanical output power of the motor. $P_{in,Electrical}$ is the electrical input power to the motor.

2.5.4 Torque (T) - current (I) relationship for PMSM (Eq. 20):

$$T = k_{torue} \times I \tag{20}$$

Where, k_{torue} is the torque constant of the PMSM.

2.5.5 Mechanical power ($P_{Mechanical}$) (Eq. 21):

$$P_{Mechanical} = T \times \omega \tag{21}$$

Where, ω is the angular velocity of the motor.

2.5.6 DC-AC conversion power losses (Eq. 22):

$$P_{Loss,DC-AC} = P_{in,DC} - P_{out,AC} \tag{22}$$

2.5.7 DC-DC conversion power losses (Eq. 23):

$$P_{Loss,DC-DC} = P_{in,Battery} - P_{out,DC} \tag{23}$$

3. Results and Discussion

3.1 EV Charging used with Modular Four-Channel 50 kW WPT System uses a Vienna Rectifier

The modular four-channel 50 kW WPT system uses a Vienna rectifier to convert grid AC power to DC power while maintaining power factor. Vienna rectifiers, noted for their efficiency and harmonic distortion reduction, can handle 230 V grid power and 30 A current. MATLAB/Simulink showed that the Vienna rectifier converted three-phase AC input to steady DC output as shown in Figure 6. The system was configured to handle typical power supply circumstances for rapid EV charging stations with input grid voltage (230 V) and current (30 A). The Vienna rectifier maintained a high-power factor near to unity in simulations, which is essential for power system efficiency and loss reduction. The Vienna rectifier's DC output voltage was stabilised at a higher voltage for the WPT system's inverter and transformer stages to ensure smooth power transmission. Vienna rectifier DC output voltage was about 800 V, meeting cascade full-bridge inverter and WPT system operating requirements. The high DC voltage allows the inverter to effectively work at 86 kHz, boosting the voltage for wireless power transmission. The Vienna rectifier's input current has minimal total harmonic distortion (THD), indicating its efficacy in boosting grid power. This is essential for regulatory compliance and power conversion process reliability and efficiency. The simulation showed that the rectifier can manage rapid EV charging power levels with a steady-state output current that meets the system's design. The rectifier's excellent power conversion and stabilisation helps the WPT system supply high power to the load. Finally, the Vienna rectifier's integration with the modular four-channel 50 kW WPT system is crucial to converting grid AC power to DC efficiently and with power factor adjustment. It can provide a steady 800 V DC output voltage, 230 V input grid

voltage and 30 A current, according to simulations. This increases WPT system efficiency and reliability, allowing rapid and efficient EV charging.

The study primarily relies on simulation data to demonstrate the effectiveness of the modular four-channel 50 kW WPT system. 3-D finite element method (FEM) simulations were used to validate the decoupled coil design, showing minimal interference between channels and balanced misalignment tolerance. Additionally, MATLAB/Simulink simulations confirmed that the system achieves 50.8 kW power output with 97% DC-to-DC efficiency over a 200 mm air gap. The misalignment performance analysis demonstrated that the system maintains 94.8% efficiency at 150 mm misalignment and 89.9% at 300 mm, proving its robustness compared to single-channel WPT systems.

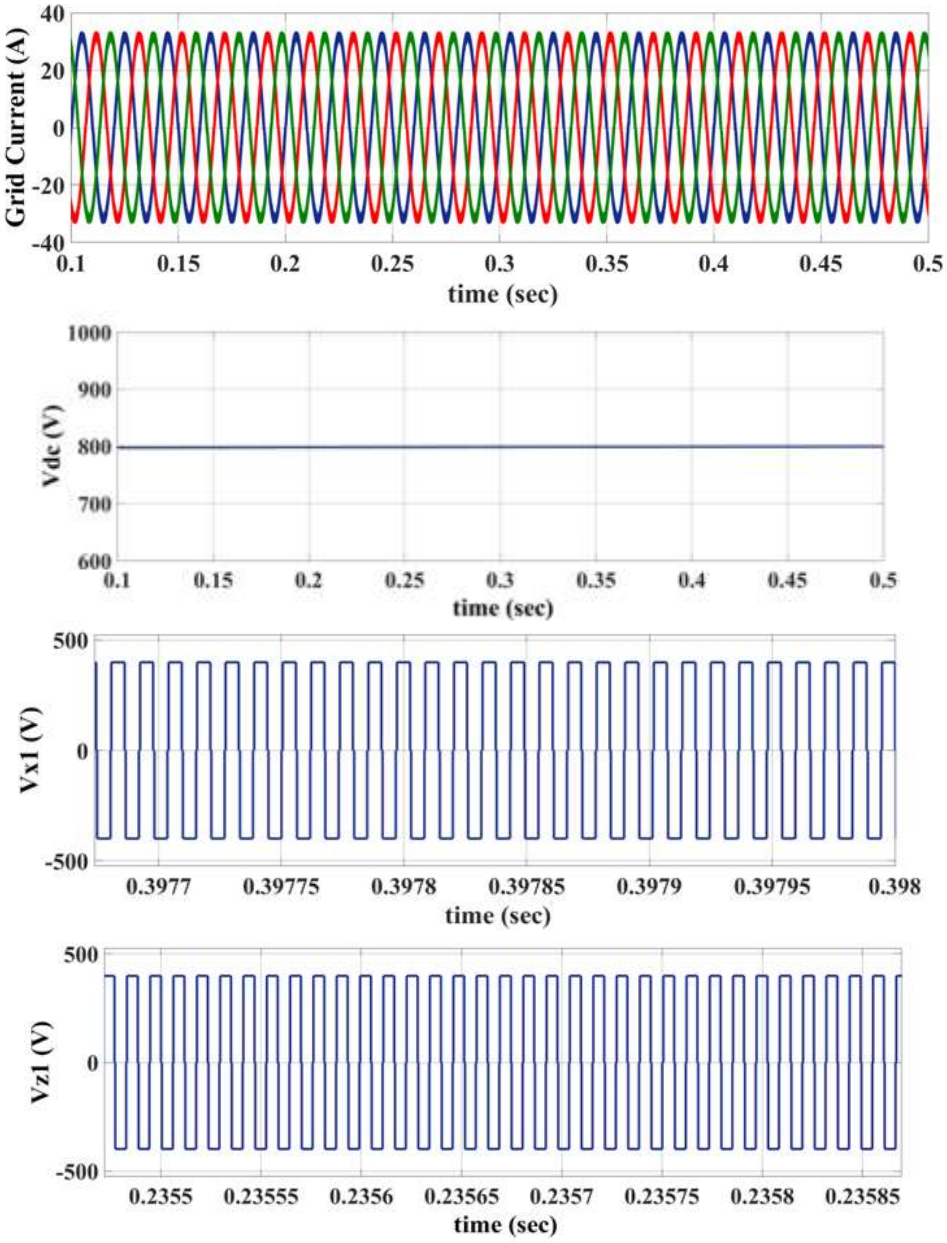

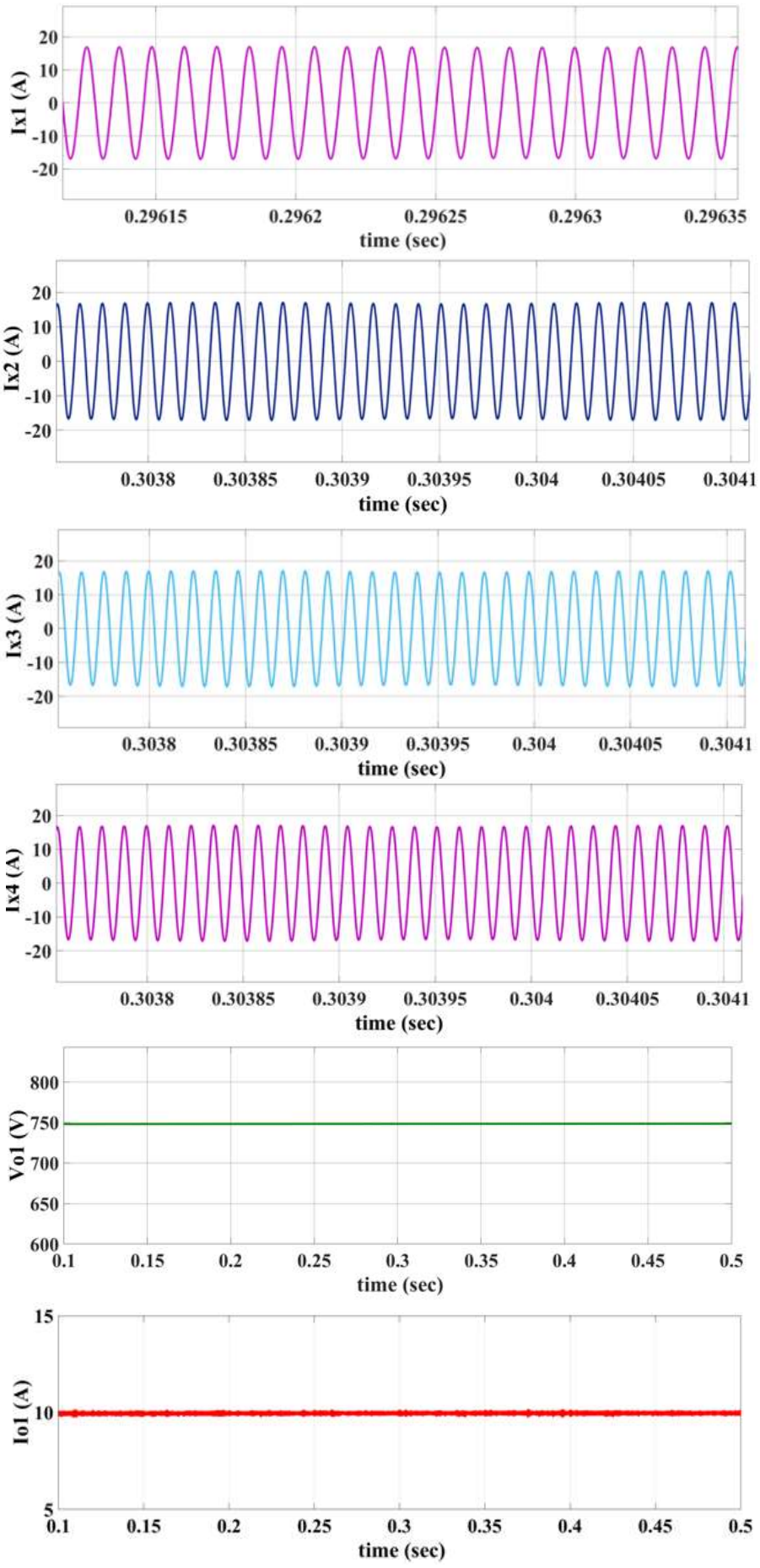
Ix1 (A)
20
10
0
-10
-20
0.29615
0.2962
0.29625
0.2963
0.29635
time (sec)
Ix2 (A)
20
10
0
-10
-20
0.3038
0.30385
0.3039
0.30395
0.304
0.30405
0.3041
time (sec)
Ix3 (A)
20
10
0
-10
-20
0.3038
0.30385
0.3039
0.30395
0.304
0.30405
0.3041
time (sec)
Ix4 (A)
20
10
0
-10
-20
0.3038
0.30385
0.3039
0.30395
0.304
0.30405
0.3041
time (sec)
Vo1 (V)
800
750
700
650
600
0.1
0.15
0.2
0.25
0.3
0.35
0.4
0.45
0.5
time (sec)
Io1 (A)
15
10
5
0.1
0.15
0.2
0.25
0.3
0.35
0.4
0.45
0.5
time (sec)

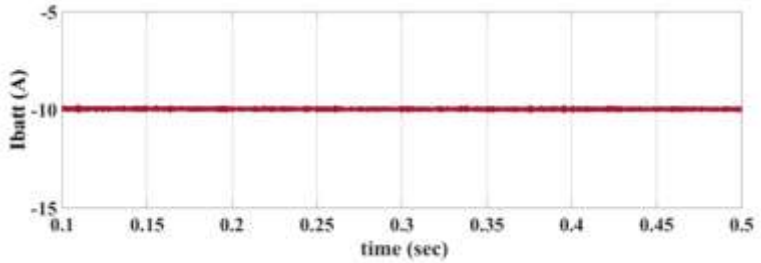

Fig. 6. Waveform when four channels are fully loaded

The integration and simulation of the modular four-channel 50 kW WPT system were meticulously carried out using MATLAB/Simulink, emphasizing the system's performance and reliability. The design includes a cascade full-bridge inverter operating at a frequency of 86 kHz and the simulation results underscore the system's efficacy in high-power transfer applications. The primary voltage (Vx1) of the transformer was recorded at 400 V, while the primary current (Ix1) measured 20 A. These values indicate that the transformer is efficiently stepping up the voltage to the required level while maintaining a manageable current. This efficient voltage transformation is critical for ensuring that the WPT system can deliver high power without incurring excessive losses or encountering thermal issues. The four-channel design of the WPT system demonstrated consistent performance, with each channel (Ix2, Ix3, Ix4) carrying a current of 20 A. This uniform current distribution across all channels is a testament to the system's balanced power handling capabilities. Such uniformity is essential for the stability and reliability of the system, as it prevents overloading of individual channels and ensures even power distribution as shown in Figure 6. At the load end, the system successfully delivered a voltage (Vo1) of 750 V and a current (Io1) of 10 A. These load conditions confirm that the WPT system can effectively transfer power to the load with high efficiency. The high load voltage and current are indicative of the system's ability to meet the demands of fast EV charging, providing sufficient power to quickly recharge EV batteries. The results from the simulation validate the modular four-channel design's capability to manage high power levels efficiently. The decoupled coil design within the WPT system minimizes cross-coupling effects, leading to more efficient power transfer and reducing potential interference between channels. The system's high-frequency operation at 86 kHz further enhances power transfer efficiency, making it well-suited for practical implementation in fast EV charging infrastructure. The successful simulation outcomes demonstrate that the proposed system not only meets but exceeds the necessary performance metrics for modern EV charging. It offers a robust solution capable of delivering high power in a stable, efficient manner, addressing key challenges such as voltage stress, insulation requirements and cross-channel interference. These results provide a strong foundation for the future development and deployment of high-power WPT systems in the EV industry, highlighting the potential for significant advancements in charging technology and efficiency.

3.2 Different Speed Variation of PMSM Drive Application

EV battery systems include a sophisticated system called the PMSM drive, which relies on power electronics to transform the DC current from the battery into the AC current needed, as seen in Figure 7. This transformation is made possible by an inverter, which transforms the direct current (DC) electricity from the battery into alternating current (AC) in three phases. Through the use of sensors, the PMSM drive's control system keeps tabs on critical parameters such as motor speed, position and current, feeding this information back into the control algorithm in real time. Motor speed, torque and rotational direction may be precisely controlled by the control algorithm, which modulates the

AC power supply's frequency, voltage and phase angle. In response to input from the PMSM drive, which provides both power and control signals, the motor spins, which causes the vehicle's wheels to turn. Optimal performance, efficiency and dependability are guaranteed by the PMSM drive, which continually modifies its control signals depending on data from the motor sensors. Ensuring smooth acceleration, deceleration and overall vehicle functioning is this closed-loop control system. Figure 7 displays the results of the simulation, which showcase the control system's ability to maintain constant performance by showing how the speed of the PMSM drive varies under different load circumstances. To top it all off, the PMSM drive is perfect for electric cars that need accurate and dynamic control of motor functions because of how fast it can react to changes in operating circumstances.

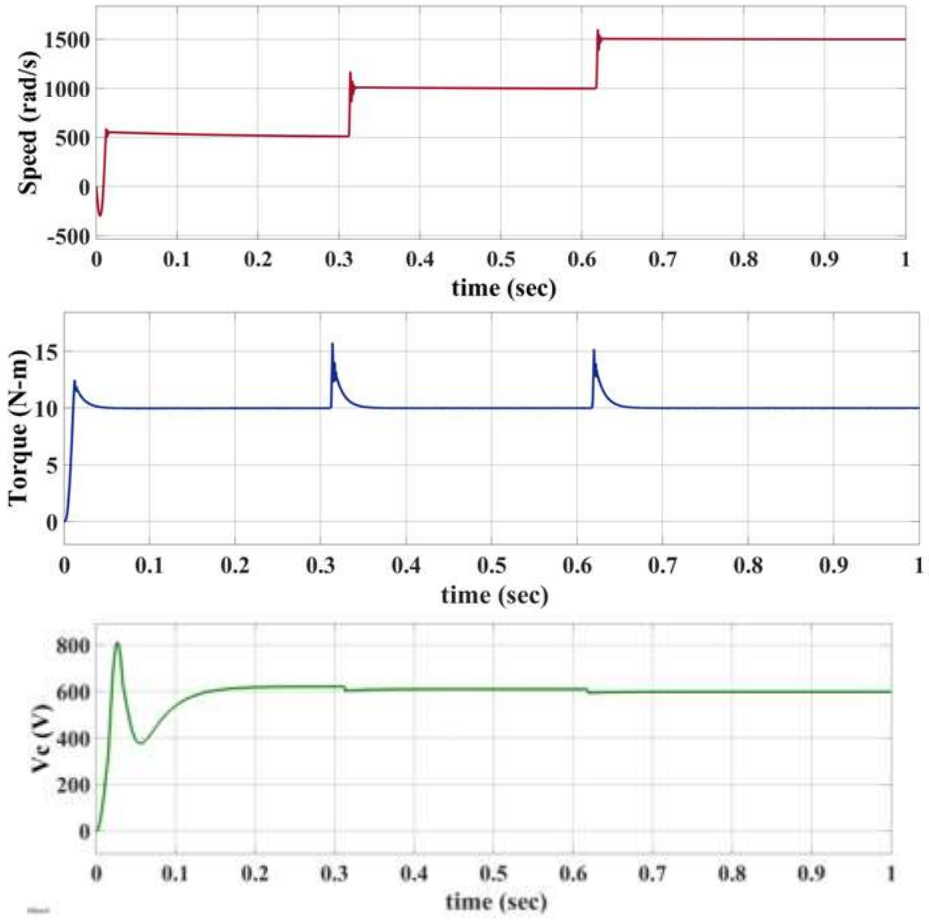

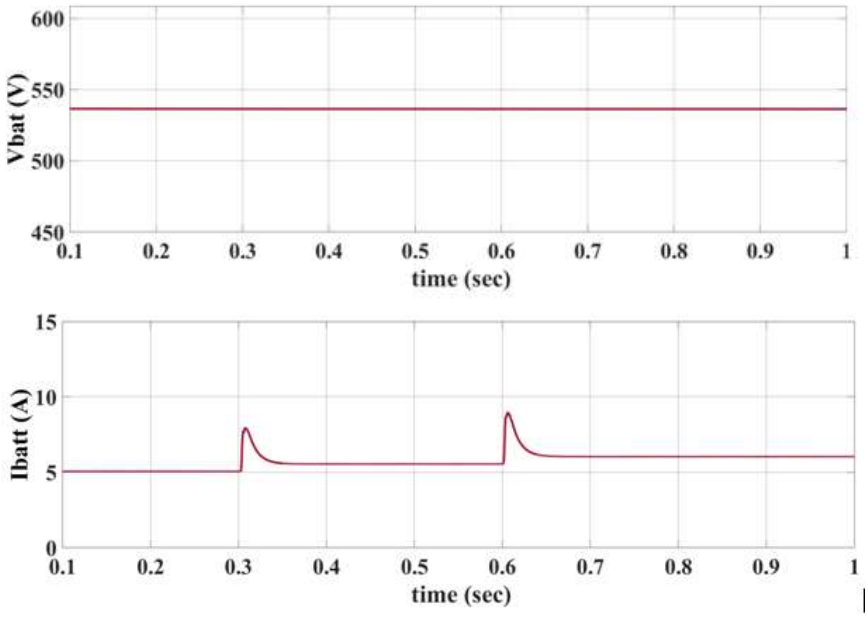

Fig. 7. Simulation results of different speed variation PMSM drive

The quantitative analysis of the modular four-channel 50 kW WPT system demonstrates its robust misalignment tolerance, making it highly suitable for real-world EV charging. At 0 mm misalignment, the system achieves 50.8 kW output power with 97% DC-to-DC efficiency and a coupling coefficient (k) of 0.261. Even with a 150 mm lateral or vertical misalignment, power transfer remains efficient at 23.7 kW with 94.8% efficiency, while the coupling coefficient drops moderately to 0.19. At 300 mm misalignment, the system still delivers 10.5 kW power with 89.9% efficiency, proving its ability to function effectively despite significant misalignment. Compared to traditional single-channel WPT systems, which typically fail beyond 100 mm misalignment, the proposed system's rotationally symmetric four-channel magnetic coupler ensures balanced power transfer in both lateral and vertical directions, reducing the need for precise EV parking alignment. These results confirm that the decoupled coil architecture enhances power transfer reliability, scalability and practicality, making it a superior solution for fast and efficient wireless EV charging.

4. Conclusion

The modular four-channel 50 kW WPT system represents a significant advancement in fast EV charging by integrating a decoupled coil design that enhances power transfer capabilities while addressing challenges such as voltage stress, insulation constraints and cross-coupling effects. Its modular architecture ensures balanced misalignment tolerance, making it highly suitable for real-world EV parking scenarios. Compared to traditional single-channel WPT systems, this approach minimizes coil interference, improves power transfer balance and enhances scalability, leading to more efficient and reliable operation. Additionally, the seamless integration of the PMSM drive with the EV battery system improves vehicle efficiency and performance, with energy regeneration during braking extending the driving range and reducing reliance on larger battery sizes. The study's findings confirm that the system delivers 50.8 kW power with 97% DC-to-DC efficiency over a 200 mm airgap, supporting its high-power capabilities and operational reliability. The symmetry and rotational design of the four-channel magnetic coupler further enhance practicality and user-friendliness, ensuring consistent power transfer under different misalignment conditions. Future research will focus on

optimizing PMSM design and control strategies, refining multi-channel synchronization and improving coil power density to further advance EV charging and propulsion technologies.

Acknowledgement
This research was not funded by any grant.

References
[1] Patil, Devendra, Matthew K. McDonough, John M. Miller, Babak Fahimi and Poras T. Balsara. "Wireless power transfer for vehicular applications: Overview and challenges." *IEEE Transactions on Transportation Electrification* 4, no. 1 (2017): 3-37. https://doi.org/10.1109/TTE.2017.2780627

[2] Veerendra, Arigela Satya, Kumaran Kadirgama, Sivayazi Kappagantula and Subbarao Mopidevi. "An MPPT controller with a modified four-leg interleaved DC/DC boost converter for fuel cell applications." *Journal of Advanced Research in Applied Sciences and Engineering Technology* 53, no. 1 (2025): 219. https://doi.org/10.37934/araset.53.1.219236

[3] Azmar, Nur Amira Syahirah and Raja Noor Farah Azura Raja Ma. "Towards Sustainable Mobility: Identifying Ideal Locations for Photovoltaic Electric Charging Stations (PEVCS) in Malaysia." *Journal of Advanced Research Design* 111, no. 1 (2023): 1-8. https://doi.org/10.37934/ard.111.1.18

[4] Foote andrew and Omer C. Onar. "A review of high-power wireless power transfer." In *2017 IEEE Transportation Electrification Conference and Expo (ITEC)*, pp. 234-240. IEEE, 2017. https://doi.org/10.1109/ITEC.2017.7993277

[5] Miller, John M. and Andrew Daga. "Elements of wireless power transfer essential to high power charging of heavy duty vehicles." *IEEE Transactions on Transportation Electrification* 1, no. 1 (2015): 26-39. https://doi.org/10.1109/TTE.2015.2426500

[6] Hao, Hao, Grant A. Covic and John T. Boys. "A parallel topology for inductive power transfer power supplies." *IEEE Transactions on Power Electronics* 29, no. 3 (2013): 1140-1151. https://doi.org/10.1109/TPEL.2013.2262714

[7] Pries, Jason, Veda Prakash Nagabhushana Galigekere, Omer C. Onar and Gui-Jia Su. "A 50-kW three-phase wireless power transfer system using bipolar windings and series resonant networks for rotating magnetic fields." *IEEE Transactions on Power Electronics* 35, no. 5 (2019): 4500-4517. https://doi.org/10.1109/TPEL.2019.2942065

[8] Galigekere, Veda Prakash, Jason Pries, Omer C. Onar, Gui-Jia Su, Saeed Anwar, Randy Wiles, Larry Seiber and Jonathan Wilkins. "Design and implementation of an optimized 100 kW stationary wireless charging system for EV battery recharging." In *2018 IEEE Energy Conversion Congress and Exposition (ECCE)*, pp. 3587-3592. IEEE, 2018. https://doi.org/10.1109/ECCE.2018.8557590

[9] Bosshard, Roman and Johann W. Kolar. "Multi-objective optimization of 50 kW/85 kHz IPT system for public transport." *IEEE Journal of Emerging and Selected Topics in Power Electronics* 4, no. 4 (2016): 1370-1382. https://doi.org/10.1109/JESTPE.2016.2598755

[10] Li, Yong, Ruikun Mai, Mingkai Yang and Zhengyou He. "Cascaded multi-level inverter based IPT systems for high power applications." *Journal of Power Electronics* 15, no. 6 (2015): 1508-1516. https://doi.org/10.6113/JPE.2015.15.6.1508

[11] Nguyen, Bac Xuan, D. M. Vilathgamuwa, Gilbert Foo andrew Ong, Prasad K. Sampath and Udaya K. Madawala. "Cascaded multilevel converter based bidirectional inductive power transfer (BIPT) system." In *2014 International Power Electronics Conference (IPEC-Hiroshima 2014-ECCE ASIA)*, pp. 2722-2728. IEEE, 2014. https://doi.org/10.1109/IPEC.2014.6869975

[12] Rahnamaee, Hamid Reza, Udaya K. Madawala and Duleepa J. Thrimawithana. "A multi-level converter for high power-high frequency IPT systems." In *2014 IEEE 5th International Symposium on Power Electronics for Distributed Generation Systems (PEDG)*, pp. 1-6. IEEE, 2014. https://doi.org/10.1109/PEDG.2014.6878623

[13] Rahnamaee, Hamid Reza, Duleepa J. Thrimawithana and Udaya K. Madawala. "MOSFET based Multilevel converter for IPT systems." In *2014 IEEE international conference on industrial technology (ICIT)*, pp. 295-300. IEEE, 2014. https://doi.org/10.1109/ICIT.2014.6894883

[14] Deng, Qijun, Pan Sun, Wenshan Hu, Dariusz Czarkowski, Marian K. Kazimierczuk and Hong Zhou. "Modular parallel multi-inverter system for high-power inductive power transfer." *IEEE Transactions on Power Electronics* 34, no. 10 (2019): 9422-9434. https://doi.org/10.1109/TPEL.2019.2891064

[15] Ahn, Dukju and Songcheol Hong. "Effect of coupling between multiple transmitters or multiple receivers on wireless power transfer." *IEEE Transactions on Industrial Electronics* 60, no. 7 (2012): 2602-2613. https://doi.org/10.1109/TIE.2012.2196902

[16] Johari, Rizal, James V. Krogmeier and David J. Love. "Analysis and practical considerations in implementing multiple transmitters for wireless power transfer via coupled magnetic resonance." *IEEE Transactions on Industrial Electronics* 61, no. 4 (2013): 1774-1783. https://doi.org/10.1109/TIE.2013.2263780
[17] Li, Yong, Tianren Lin, Ruikun Mai, Limin Huang and Zhengyou He. "Compact double-sided decoupled coils-based WPT systems for high-power applications: Analysis, design and experimental verification." *IEEE Transactions on Transportation Electrification* 4, no. 1 (2017): 64-75. https://doi.org/10.1109/TTE.2017.2745681
[18] Shijo, Tetsu, Kenichirou Ogawa, Masatoshi Suzuki, Yasuhiro Kanekiyo, Masaaki Ishida and Shuichi Obayashi. "EMI reduction technology in 85 kHz band 44 kW wireless power transfer system for rapid contactless charging of electric bus." In *2016 IEEE Energy Conversion Congress and Exposition (ECCE)*, pp. 1-6. IEEE, 2016. https://doi.org/10.1109/ECCE.2016.7855077
[19] Liu, Hang, Qianhong Chen, Guangjie Ke, Xiaoyong Ren and Siu-Chung Wong. "Research of the input-parallel output-series inductive power transfer system." In *2015 IEEE PELS Workshop on Emerging Technologies: Wireless Power (2015 WoW)*, pp. 1-7. IEEE, 2015. https://doi.org/10.1109/WoW.2015.7132802
[20] Murshid, Shadab and Bhim Singh. "Implementation of PMSM drive for a solar water pumping system." *IEEE Transactions on Industry Applications* 55, no. 5 (2019): 4956-4964. https://doi.org/10.1109/TIA.2019.2924401
[21] Antonello, Riccardo, Matteo Carraro, Alessandro Costabeber, Fabio Tinazzi and Mauro Zigliotto. "Energy-efficient autonomous solar water-pumping system for permanent-magnet synchronous motors." *IEEE Transactions on Industrial Electronics* 64, no. 1 (2016): 43-51. https://doi.org/10.1109/TIE.2016.2595480
[22] Brinner, Thomas R., Robert H. McCoy and Trevor Kopecky. "Induction versus permanent-magnet motors for electric submersible pump field and laboratory comparisons." *IEEE Transactions on industry applications* 50, no. 1 (2013): 174-181. https://doi.org/10.1109/TIA.2013.2288203
[23] Wilamowski, Bogdan M. and J. David Irwin, eds. *Power electronics and motor drives*. CRC press, 2018. https://doi.org/10.1201/9781315218410
[24] Niu, Feng, Kui Li and Yao Wang. "Direct torque control for permanent-magnet synchronous machines based on duty ratio modulation." *IEEE Transactions on Industrial Electronics* 62, no. 10 (2015): 6160-6170. https://doi.org/10.1109/TIE.2015.2426678
[25] Vafaie, Mohammad Hossein, Behzad Mirzaeian Dehkordi, Payman Moallem and Arash Kiyoumarsi. "Minimizing torque and flux ripples and improving dynamic response of PMSM using a voltage vector with optimal parameters." *IEEE Transactions on industrial electronics* 63, no. 6 (2015): 3876-3888. https://doi.org/10.1109/TIE.2015.2497251
[26] Kim, Won-Jae and Sang-Hoon Kim. "A sensorless V/F control technique based on MTPA operation for PMSMs." In *2018 IEEE Energy Conversion Congress and Exposition (ECCE)*, pp. 1716-1721. IEEE, 2018. https://doi.org/10.1109/ECCE.2018.8557412
[27] Zhang, Zhenrui, Haohao Guo, Yancheng Liu, Qiaofen Zhang, Pengli Zhu and Rashid Iqbal. "An improved sensorless control strategy of ship IPMSM at full speed range." *IEEE Access* 7 (2019): 178652-178661. https://doi.org/10.1109/ACCESS.2019.2958650
[28] Hang, Jun, Mengjie Xia, Shichuan Ding, Yuanqi Li, Le Sun and Qunjing Wang. "Research on vector control strategy of surface-mounted permanent magnet synchronous machine drive system with high-resistance connection." *IEEE Transactions on Power Electronics* 35, no. 2 (2019): 2023-2033. https://doi.org/10.1109/TPEL.2019.2918683
[29] Gong, Chao, Yihua Hu, Jinqiu Gao, Yangang Wang and Liming Yan. "An improved delay-suppressed sliding-mode observer for sensorless vector-controlled PMSM." *IEEE Transactions on Industrial Electronics* 67, no. 7 (2019): 5913-5923. https://doi.org/10.1109/TIE.2019.2952824
[30] Kolar, Johann W., Hans Ertl and Franz C. Zach. "Design and experimental investigation of a three-phase high power density high efficiency unity power factor PWM (VIENNA) rectifier employing a novel integrated power semiconductor module." In *Proceedings of Applied Power Electronics Conference. APEC'96*, vol. 2, pp. 514-523. IEEE, 1996. https://doi.org/10.1109/APEC.1996.500491
[31] Kolar, Johann W., Uwe Drofenik and F. C. Zach. "Current handling capability of the neutral point of a three-phase/switch/level boost-type PWM (VIENNA) rectifier." In *PESC Record. 27th Annual IEEE Power Electronics Specialists Conference*, vol. 2, pp. 1329-1336. IEEE, 1996. https://doi.org/10.1109/PESC.1996.548754
[32] Qiao, Chongming and Keyue M. Smedley. "Three-phase unity-power-factor VIENNA rectifier with unified constant-frequency integration control." In *7th IEEE International Power Electronics Congress. Technical Proceedings. CIEP 2000 (Cat. No. 00TH8529)*, pp. 125-130. IEEE, 2000. https://doi.org/10.1109/CIEP.2000.891402
[33] Kolar, Johann W. and Franz C. Zach. "A novel three-phase utility interface minimizing line current harmonics of high-power telecommunications rectifier modules." *IEEE Transactions on Industrial Electronics* 44, no. 4 (2002): 456-467. https://doi.org/10.1109/41.605619